DOI: 10.26599/FSHW.2025.9250852

Y.M. Zhang et al. / Food Science and Human Wellness 16 (2027)

Contents lists available at SciOpen

Food Science and Human Wellness

journal homepage: https://www.sciopen.com/journal/2097-0765

China Food Publishing Co.

Ketogenic diet disrupts BDH1-mediated ketone metabolism and causes myocardial dysfunction in mice

Yin Li[a, b, c, *], Bin Guo[d, *], Hui Shu[b], Hongyu Fu[b], Xiangpeng Liu[b], Jie Zhang[b], Yue Ma[b], Zhiwei Liu[b], Lei Fu[d], Yingying Dong[b], Xiaobo Sun[e, f, g], Bin Zhang[e, f, g], Zhihao Jia[b], Xiaosong Gu[h, #], Hong Sun[i, #], Yu Feng[a, j, #]

[a] *Department of Rheumatology and Immunology, The Fourth Affiliated Hospital of Soochow University, Medical Center of Soochow University, Suzhou Dushu Lake Hospital, Suzhou 215123, China*

[b] *Cambridge-Suda Genomic Resource Center, Suzhou Medical College, Soochow University, Suzhou 215123, China*

[c] *School of life science, Suzhou Medical College, Soochow University, Suzhou 215123, China*

[d] *Wisdom Lake Academy of Pharmacy, Xi'an Jiaotong-Liverpool University, Suzhou 215123, China*

[e] *Institute of Medicinal Plant Development, Peking Union Medical College and Chinese Academy of Medical Sciences, Beijing 100193, China*

[f] *Key Laboratory of Bioactive Substances and Resources Utilization of Chinese Herbal Medicine, Ministry of Education, Beijing 100193, China*

[g] *Beijing Key Laboratory of Innovative Drug Discovery of Traditional Chinese Medicine (Natural Medicine) and Translational Medicine, Beijing 100193, China*

[h] *Department of Cardiology, the Second Affiliated Hospital of Soochow University, 215004, Suzhou City, Jiangsu Province, China*

[i] *Department of Endocrinology and Metabolism, The Fourth Affiliated Hospital of Soochow University, Suzhou Dushu Lake Hospital, Medical Center of Soochow University, Suzhou, 215123, Jiangsu, China*

[j] *Department of Endocrinology, The Second Affiliated Hospital of Soochow University, Suzhou 215123, China*

ABSTRACT: Ketogenic diet (KD), recognized for its multiple metabolic benefits, such as enhanced glycemic homeostasis and weight loss, also imposes intricate influences on cardiac substrate utilization. While KD is effective in reducing blood glucose levels and improving insulin sensitivity, its long-term effects on myocardial ketone body (KB) metabolism remain insufficiently investigated, particularly in relation to cardiac remodeling. In the present study, we found that the KD-based nutritional intervention caused considerable cardiac hypertrophy, altered FAs and KBs metabolic pathways and impaired cardiac function, potentially through the repression of BDH1 protein, which is crucial for the utilization of β-hydroxybutyrate (β-OHB). Additionally, mice with cardiac muscle-specific *Bdh1* manipulation exhibited cardiac dysfunction after fasting, possibly due to histone methylation modifications. We established several diabetic models using streptozotocin (STZ), *db/db* transgenic mice, and a combination of STZ and a high-fat diet (HFD). We confirmed that these diabetic models exhibited significant alterations in cardiac ketone body metabolism and BDH1 expression. In summary, our study highlights that the downregulation of BDH1 induced by the ketogenic diet is associated with disrupted myocardial ketone utilization and may lead to myocardial structure and function impairment. Furthermore, the loss of BDH1 can also aggravate cardiac dysfunction during fasting by histone modifications.

Keywords: Ketogenic diet, Cardiomyopathy, BDH1, Ketone metabolism, Diabetes

***Equal contribution**

[#] To whom correspondence should be addressed
xiaosonggu@hotmail.com (Gu, Xiaosong); sunhong_611@126.com (Sun, Hong); fengyu1980@suda.edu.cn (Feng, Yu)

Received 24 January 2025
Received in revised from 6 March 2025
Accepted 3 April 2025

1. Introduction

Ketogenic diet (KD), typically characterized by high fat intake and very low carbohydrates, has been widely implemented in the management of metabolic diseases, particularly type 2 diabetes mellitus (T2DM), obesity, and metabolic syndrome[1]. By promoting hepatic ketogenesis and suppressing insulin secretion, KD has demonstrated clinical benefits such as improved glycemic control, enhanced insulin sensitivity, and favorable lipid remodeling in obese and insulin-resistant individuals[1, 2]. Beyond metabolic regulation, KD also exerts broader systemic effects, ranging from supporting mitigating inflammation to enhancing neurological function and possibly offering protective effects against certain cancers[3-5]. As a popular dietary strategy, KD is increasingly incorporated into lifestyle interventions aimed at improving metabolic health, making it critical to evaluate its overall safety and potential untoward effects on vital organs, including the heart. Despite these recognized advantages, its long-term cardiac effects remain a matter of debate[6], it remains uncertain whether these metabolic advantages fully extend to the long-term preservation of cardiac function, especially given that high circulating lipids and ketone bodies (KBs) may differentially affect myocardial energy metabolism under various physiological and pathological conditions

Heart, due to its consistent action, requires considerable energy input. In normal heart, it obtains adenosine triphosphate (ATP) from sources including glucose (20% - 40% of ATP), free fatty acids (FFAs, 40% - 60% of ATP), ketone bodies (KBs, 10% - 15% of ATP), pyruvate, and amino acids [7-11]. The myocardium undergoes notable metabolic perturbations during heart failure (HF), shifting away from fatty acid oxidation toward greater utilizaticon of alternative substrates, such as glucose, lactate, and ketone bodies. Increasing evidence from both experimental and clinical studies indicates that this enhanced reliance on ketone bodies may serve as an adaptive mechanism, potentially offering metabolic and functional benefits for the failing heart. [12-15]. This advantage is potentially due to the higher energy efficiency of KBs compared to glucose, as they may deliver a modestly greater free-energy yield per unit of oxygen than either glucose or long-chain fatty acids[16-18]. Notably, β-hydroxybutyrate (β-OHB), the predominant and more stable ketone body in circulation, is reversibly converted from acetoacetate (AcAc) by the mitochondrial enzyme BDH1 (3-hydroxybutyrate dehydrogenase 1), which plays a central role in ketolysis and ketogenesis[16, 19]. Conversely, research in chronic HF patients has indicated a direct relationship between elevated KB levels, the severity of the disease, and a less favorable prognosis [20-22]. Similarly, in arrhythmogenic cardiomyopathy (AC), plasma β-hydroxybutyrate (β-OHB), the predominant circulating ketone body, was significantly elevated in patients who experienced major adverse cardiac events, indicating a potentially pathogenic rather than exclusively adaptive role for elevated ketones in certain cardiac conditions[22]. Such opposing findings underscore the complexity of KD-driven ketosis, suggesting that while KBs may provide an efficient fuel for some cardiac pathologies, excessive or prolonged elevation of circulating ketones, especially in the context of high fat consumption, could pose risks to myocardial health. However, the precise contribution of BDH1 to cardiac ketone metabolism under ketogenic and diabetic conditions remains incompletely understood. In this

study, we aim to define the role of BDH1 in mediating myocardial adaptation to KD and characterize its involvement in cardiac dysfunction, metabolic remodeling, and epigenetic regulation.

In this study, we implemented KD intervention to induce elevated circulating KB levels, evaluating its implications on cardiac function and the molecular regulation of myocardial KB metabolism. Our observations uncovered that KD manipulation suppressed the expression level of BDH1 (3-hydroxybutyrate dehydrogenase 1) in cardiac tissue. To further decipher the potential role of BDH1 in dictating cardiac function, we established a global *Bdh1* knockout mouse model (*Bdh1 tm1a-/-*) and a cardiac-specific *Bdh1* knockout mouse model ($Bdh1^{MKO}$). Finally, we utilized streptozotocin (STZ)-induced T1DM models, transgenic *db/db* mice, and a combination of a high-fat diet (HFD) with STZ induction for T2DM to probe the alterations in KB metabolism and BDH1 expression under diabetic conditions. Our findings indicate that a KD, compounded by BDH1 inhibition, disrupts cardiac ketone metabolism and precipitates abnormal myocardial remodeling and function reminiscent of heart failure, suggesting that KD is not uniformly beneficial for cardiac health and that BDH1-dependent ketolysis may be an important therapeutic target when designing metabolic interventions for diabetes and other conditions involving ketosis.

2. Material and Methods

2.1 KD Intervention and model construction

KD intervention was conducted using adult C57BL/6N male mice, whereby they were provided with either a standard chow diet (control) or a KD with specific nutritional composition. The KD, adhering to established guidelines, was formulated with high-fat sources such as soybean oil or cocoa butter, minimal carbohydrate content, and balanced protein levels. The precise percentages of macronutrients and caloric content were meticulously calculated based on standardized KD protocols for rodent models (Cat#D10070801, Research Diets), with their detailed macronutrient compositions summarized in Table 1

Table 1 Nutritional composition and ingredient of the KD (Cat#D10070801)

Macronutrient	**Gm (%)**	**Kcal (%)**
Protein	17	10
Carbohydrate	0.2	0
Fat	67	90
Total	—	100
kcal/gm	6.7	—
Ingredient	**Gm**	**Kcal**
Casein	100	400
L-Cystine	1.5	6
Cellulose, BW200	50	0
Soybean Oil	25	225
Cocoa Butter	381	3429
Mineral Mix, S10026	10	0
DiCalcium Phosphate	13	0
Calcium Carbonate	5.5	0
Potassium Citrate, 1 H2O	16.5	0
Vitamin Mix, V10001C	1	4
Choline Bitartrate	2	0

FD&C Yellow Dye #5	0.025	0
FD&C Red Dye #40	0.025	0
FD&C Blue Dye #1	0	0
Total	605.5	4064

2.2 Diabetic animal models

Mice of the C57BL/6N lineage, used to model diabetic conditions, were either bred and maintained at the Cambridge-Suda Genomic Research Center's animal facility at Soochow University (CAM-SU, Suzhou, China) or purchased from Cyagen (*db/db* transgenic mice). All mice had unrestricted access to standard rodent food (autoclaved and irradiated) and acidified water. All mouse handling and experiments were conducted following the approved animal protocols (ZJ-2021-1) for experimental mice usage, as sanctioned by the Institutional Animal Care and Use Committee of CAM-SU on December 24th, 2021.

To generate streptozotocin (STZ)-induced mouse T1DM model, adult C57BL/6N male mice were fasted overnight (from 8 p.m. to 9 a.m.) prior to STZ administration. A repeated low-dose STZ regimen was used, consisting of two intraperitoneal injections of 75 mg/kg STZ (Cat# S0130, Sigma-Aldrich), administered 48 hours apart, freshly dissolved in a citrate buffer with a pH of 4.5. Following STZ administration, mice were given unrestricted access to food and water. Within a span of 72 h post-STZ injection, blood glucose levels were ascertained using a glucometer (Performa, ACCU-CHEK). Instances wherein glucose levels exceeded 16.7 mmol were indicative of a successful T1DM induction and said subjects were further utilized for study.

To mimic T2DM conditions, adult C57BL/6N male mice were subjected to a high-fat diet (HFD, 60% calories from fat) for a preliminary 4-week period. The diet, inducing rapid weight gain and insulin impairment, effectively established a pre-diabetic state in the subjects. Following the HFD feeding period, a carefully measured dose of 75 mg/kg of STZ, freshly dissolved in citrate buffer with a pH of 4.5, was administered via intraperitoneal injection. A fasting period of overnight, directly prior to STZ administration, aided in depleting endogenous insulin levels. After the STZ injection, the mice were given unrestricted access to the HFD and water. 72 h post-STZ administration, a glucometer audit of blood glucose levels was conducted. Mice with glucose levels exceeding 16.7 mmol were classified as diabetic and consequently utilized for further study.

2.3 Body composition measurement

The Minispec body composition analyzer (LF50, Bruker) was employed to assess the total body fat mass and lean mass of the live mice without the need for anesthesia. Briefly, the mice were positioned within a clear plastic container, which was inserted into the designated section of the Minispec LF50 system. Durability of the scan's precision required the mice to remain immobile within this custom-sized container for the duration of the process.

2.4 Indirect calorimetry measurement

Using the Oxymax indirect calorimetry system (CLAMS-16M, Columbus Instruments), we measured the oxygen consumption rate (VO_2) and carbon dioxide production rate (VCO_2). The system was maintained in a temperature-controlled setting (24 °C) with a balanced 12 h light and 12 h dark cycle (Light: 8 a.m.-8 p.m.;

Dark: 8 p.m.-8 a.m.). Throughout the procedure, each mouse was individually housed in separate chambers with unrestricted access to food and water. Before the measurements, a 24 h adjustment phase was provided for the mice in the chambers. For this study, energy expenditure data were presented without corrections. The average energy expenditures for daytime (8 a.m.-8 p.m.) and nighttime (8 p.m.-8 a.m.) were calculated based on the mean value of all data collected during each 12-hour cycle.

2.5 Cardiac functional test

The cardiac function of mice was evaluated utilizing non-invasive echocardiography. Mice were anesthetized lightly with isoflurane and positioned securely on a heated platform to maintain their body temperature. Transthoracic echocardiography (VINNO6, VINNO) was performed with a 15-17 MHz high-frequency linear transducer to capture two-dimensional and M-mode images of the left ventricle (LV) from the parasternal short-axis and long-axis views. To ensure continuous anesthesia, a nose cone was used, and hair removal cream was applied to the chest area, followed by cleaning with wet gauze to ensure complete hair removal. During the imaging process, the anesthesia level was adjusted carefully to maintain an appropriate heart rate, increasing the concentration if the mouse showed signs of waking. Ultrasound gel was applied to the imaging area to ensure full coverage between the probe and the skin. Parameters, including LV ejection fraction and indices of both systolic and diastolic function, were measured. In B-mode, the papillary muscles were aligned parallel to the screen. The M-mode button was then pressed, positioning the yellow line in the center of the left ventricle. The display window was set to 1000 ms. If the image was unclear, adjustments were made by shifting the yellow line left or right, or by repositioning the platform. Each measurement was performed by an experienced technician who was blinded to the experimental groups, and results were averaged over multiple cardiac cycles to ensure accuracy and reliability. After imaging, the mice were removed from the platform and allowed to recover on a heating pad.

2.6 Glucose tolerance test

For the glucose tolerance test (GTT), mice were fasted for 16 h prior to the experiment. Following the fasting period, each mouse received an intraperitoneal injection of glucose at a dose of 2 g/kg body weight. Tail blood glucose levels were measured at specified time points: 0-, 15-, 30-, 60-, and 120-min post-injection. Blood glucose levels were determined using a glucometer (Performa, ACUU-CHEK), and the results were recorded for further analysis to assess the glucose tolerance of the mice.

2.7 Bdh1 knockout models

The global BDH1 knockout mice (*Bdh1 tm1a-/-*) were generated on a C57BL/6N background using CRISPR/Cas9 gene-editing technology. All mice were bred and maintained at the Cambridge-Suda Genomic Research Center's animal facility at Soochow University (CAM-SU, Suzhou, China), or purchased from Cyagen. Mice had unrestricted access to standard rodent food (autoclaved and irradiated) and acidified water. All animal handling and experiments were conducted following the approved animal protocols (ZJ-2021-1)

for experimental mouse usage, as sanctioned by the Institutional Animal Care and Use Committee of CAM-SU on December 24th, 2021.

The cardiac-specific BDH1 knockout mice (*Bdh1*^{MKO}) were generated by crossing BDH1-floxed mice with mice expressing Cre recombinase under the control of the cardiac-specific α-MHC promoter. All mice were maintained in the same environment and conditions, with unrestricted access to standard rodent food and acidified water.

To investigate the cardiac function of cardiac-specific BDH1 knockout mice under fasting conditions, adult male *Bdh1*^{MKO} mice and control littermates (WT) underwent a 24 h fasting period. During this fasting period, mice were only allowed access to water.

2.8 Western blotting analysis

Total proteins were extracted using a radioimmunoprecipitation assay (RIPA) buffer (Cat#P0013K, Beyotime), enhanced with a protease inhibitor cocktail (Cat#C0001, TargetMol). Protein concentrations were determined using Pierce BCA Protein Assay Reagent A/B (Cat#23228/Cat#1859078, Thermo Scientific). Preceding Western blotting analysis, lysates were heated in SDS sample buffer for 10 min and conserved at -20℃ for subsequent use. Equal amounts of protein from each sample were loaded for electrophoresis (Cat#1658033, Bio-Rad). Protein separation was achieved via 10% SDS-PAGE and transferred onto nitrocellulose membranes (Cat#IPVH00010, Sigma), which were subsequently blocked with 5% non-fat milk in TBST (Tris-buffered saline with 1% Tween) buffer at room temperature for 1 h. Following an overnight incubation at 4℃ with the specified primary antibody: BDH1 (Boster, A09277-1), ACAT1 (CST, 44276S), HSP90 (Proteintech, 13171-1-AP), GAPDH (Proteintech, 60004-1-IG), ATGL (Proteintech, 55190-1-AP), CPT2 (CST, 52552S), PGC1α (CST, 2178S), PPARα (Proteintech, 66826-1-Ig), SDHA (Boster, A01753), PKM1/2 (CST, 3190S), PGK1 (CST, 68540S), PDHK1 (CST, 3820S), Bcl-2 (CST, 15071S), SCD (Proteintech, 28678-1-AP), DGAT2 (Proteintech, 17100-1-AP), PCK1 (Proteintech, 16754-1-AP), H3K27me3 (Abcam, ab6002), H3K27ac (Abcam, ab4729), ATP5A1 (Proteintech, 14676-1-AP), UQCRC1 (Proteintech, 21705-1-AP), SDHB (Proteintech, 10620-1-AP), and NDUFB8 (Proteintech, 14794-1-AP). After washing, membranes were washed with TBST buffer and exposed to the suitable secondary antibody at room temperature for an hour. Enhanced chemiluminescence was used for visualization (ChemiScope 6000, Clinx).

2.9 Total RNA Extraction and RNA-sequencing

Trizol reagent (Cat# 15596026, Invitrogen) was utilized for the extraction of total RNA, in adherence to the manufacturer's guidelines. Post-extraction, the purity of the RNA samples was verified using aspectrophotometer (Nanodrop 3000, Thermo Fisher Scientific), establishing an absorption ratio (260/280 nm) benchmark of 2.0.

Subsequently, total RNA samples were shipped to Azenta Life Sciences for sequencing process. Briefly, RNA libraries were prepared utilizing the TruSeq Stranded Total RNA Library Prep Kit (Cat#20020596, Illumina). The process involves the selection and fragmentation of mRNA from total RNA, followed by

cDNA synthesis, end repair, adaptor ligation, and finally, amplification to construct the cDNA library. The prepared libraries were then sequenced on the Illumina sequencing platform. Paired-end reads were generated to ensure precise and accurate mapping of the transcripts. Upon sequencing, the raw reads obtained were processed and aligned to the reference genome using Bowtie2 and TopHat. Following alignment, the mapped reads corresponding to each gene were quantified by HTSeq. Next, differential gene expression analysis was performed on the RNA-Seq data using the DESeq2 package. Genes exhibiting a false discovery rate (FDR) of less than 0.05 and an absolute fold change greater than 2 were classified as differentially expressed genes. Lastly, bioinformatics analysis was conducted on the differentially expressed genes. Enrichment analysis was executed using gene ontology (GO) and pathway analysis tool DAVID, allowing for the identification of biological themes and pathways related to ketone body metabolism and diabetic cardiomyopathy.

The processed RNA-seq datasets of mouse liver and heart following KD intervention have been deposited in the Science Data Bank under accession link: https://www.scidb.cn/en/s/ZjUzmi. All relevant differential expression results and gene-level count matrices used in the study are available in the Supplementary Tables.

2.10 Non-targeted metabolomics

Metabolic profiling analysis without targeting specific metabolites was conducted using an ultra-high performance liquid chromatography system (Vanquish Flex UHPLC system, Thermo Scientific) paired with high-resolution mass spectrometry (Q Exactive Focus, Thermo Scientific). The raw data were converted to mzXML format utilizing MSConvert in the ProteoWizard software package and then processed using XCMS for feature detection, retention time correction, and alignment. Metabolites were identified by accurate mass with a deviation of less than 30 ppm and MS/MS data, matched with databases such as HMDB (http://www.hmdb.ca), MassBank (http://www.massbank.jp/), LipidMaps (http://www.lipidmaps.org), and mzCloud (https://www.mzcloud.org). Robust LOESS signal correction was employed to normalize data and correct for any systematic biases. Following normalization, only ion peaks with relative standard deviations (RSDs) below 30% in quality control (QC) samples were retained to ensure accurate metabolite identification. Multivariate data analyses and modeling were carried out using the Ropls software (version 1.30.0). Post data scaling, models were constructed based on principal component analysis (PCA), orthogonal partial least squares discriminant analysis (OPLS-DA), and partial least squares discriminant analysis (PLS-DA). Metabolic profiles were visualized as score plots, with each point representing a sample. Corresponding loading plots and S-plots provided insight into the metabolites influencing sample clustering. All models underwent evaluation for overfitting through permutation tests. The descriptive performance of the models was determined by R2X (cumulative) and R2Y (cumulative) values, where a perfect model would have R2X (cum) = 1 and R2Y (cum) = 1. Prediction performance was measured by Q2 (cumulative), with a perfect model having Q2 (cum) = 1, and permutation tests ensured that the permuted model could not predict classes: R2 and Q2 values at the Y-axis intercept had to be lower than those of Q2 and R2 in the non-permuted model. To identify discriminating metabolites, OPLS-DA was used, employing the Variable Importance on

Projection (VIP). Significant variables for classification were discovered by applying the P value, VIP scores from OPLS-DA, and fold change (FC). Metabolites with a P value less than 0.05 and VIP values greater than 1 were considered statistically significant.

2.11 Targeted quantification of ketone bodies

Serum concentrations of β-OHB and AcAc were quantified using commercially available WST-based colorimetric assay kits (Solarbio, Cat# BC5085 for β-OHB and Cat# BC5075 for AcAc), according to the manufacturer's instructions. Briefly, 10 μL of serum was used per reaction, and measurements were performed in duplicate using a microplate reader at 450 nm. Final concentrations were calculated based on standard curves and normalized to the mean of the corresponding control group in each batch.

2.12 H&E staining

Freshly harvested liver and adipose tissues were fixed in 10% neutral buffered formalin and subsequently embedded in paraffin. Tissue sections were prepared at a thickness of 5 μm using a microtome and mounted onto glass slides. To facilitate H&E staining, the sections were deparaffinized in xylene, rehydrated through a graded alcohol series, and rinsed in distilled water. The slides were then immersed in Harris hematoxylin solution, followed by differentiation in acid alcohol and counterstaining with eosin Y solution. After dehydration through graded alcohols and clearing in xylene, the stained sections were coverslipped using mounting media. Microscopic examination of the H&E-stained liver and adipose tissue sections was performed using a fluorescent microscope (DM 6000B, Leica). Images were captured at appropriate magnifications to visualize tissue morphology.

2.13 Statistical analysis

All analytical procedures were accomplished through utilization of the two-tailed Student's t-test. All empirical data are denoted as mean ± SEM. Statistical significance was inferred from comparisons yielding *P* values of less than 0.05, 0.01, or 0.001.

3. Results

3.1 KD alters systemic metabolism of the mice

To explore the effect of KB metabolism on cardiac function, we applied mice into a recent highly anticipated ketogenic condition. As indicated by body composition measurements, mice fed with KD had more body fat mass and less lean mass comparing to the ones with a control diet without changing the body weight (Figure 1A). To reflect their ability to metabolize glucose, glucose tolerance tests were conducted. Compared to the control group, the peak blood glucose level as well as the glucose clearance indicated by area under curve (AUC) in mice fed with KD is significantly higher (Figures 2B, C), suggesting impeded initial uptake and usage of glucose. Metabolically, mice fed with KD had unchanged O_2 consumption but decreased CO_2 production, leading to the respiratory exchange ratio (RER) values near 0.7 (Figures 3D-I), suggesting that with KD, mice predominately using FFAs for fuel.

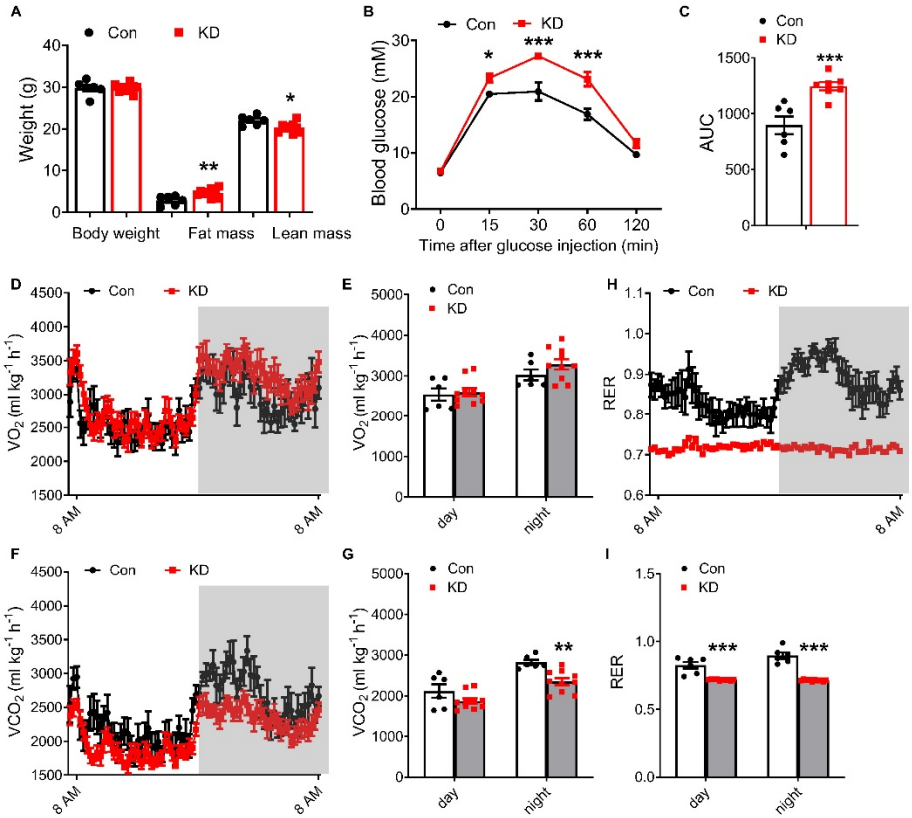

Figure 1. KD change body composition and systemic metabolism of the mice. (A) Measurements of body weight, fat mass, and lean mass. *$P < 0.05$, **$P < 0.01$ (B) Blood glucose levels after glucose injection. *$P < 0.05$, ***$P < 0.001$ (C) Area under the curve (AUC) of blood glucose levels in control (Con) and ketogenic diet (KD) mice. ***$P < 0.001$ (D-I) Oxygen consumption rate (VO_2), carbon dioxide production rate (VCO_2), and day-night oxygen consumption in control (Con) and ketogenic diet (KD) mice. **$P < 0.01$, ***$P < 0.001$. Values are mean ± SEM from, n = 6-7 (A–C) or n = 6-10 (D–G) individual mice per group.

We then isolated adipose tissues and liver from mice fed either the control or KD diet. Consistent with the increased total body fat mass, weight of epididymal white adipose tissues (eWAT), but not inguinal WAT (iWAT), was increased from KD group (Figures 2A, B). While the weight of brown adipose tissue (BAT) was significantly reduced in mice fed with KD (Figures 2A, B). Consistently, H&E staining and respective quantification revealed increases in adipocyte area of eWAT which were collected from KD group (Figures 3D, S1A). In addition, a significant reduction in liver weights and smaller hepatocyte size was observed in mice fed with KD (Figures 2C, D).

To investigate the potential reasons behind the observed decrease in liver weight, we conducted RNA-sequencing analysis on liver tissues obtained from the KD and control groups. Analysis revealed an upregulation of genes associated with KB metabolism (*Hmgcs2*, *Bdh1*, and *Acat1*), indicating the success of this ketogenic treatment (Figure 2E). In addition, the expression levels of key enzymes involved in FA synthesis, namely, *Fasn*, *Acacb*, *Elovl6*, *Acly*, and *Acaca*, were reduced (Figure 2E). GO analysis indicated that KD upregulated lipid catabolism related genes, and downregulated lipid synthesis and gluconeogenesis related genes (Figures S2A, B). We next conducted western blotting analyses to verify the RNA-sequencing data. The results demonstrated significant increases in the protein levels of BDH1 and ACAT1, essential enzymes involved in KB metabolism, as well as ATGL and CPT2, crucial for lipolysis and FA β-oxidation (Figure 2F). In the meanwhile, the level of protein involved in glycolysis, including GAPDH, was

significantly decreased (Figure 2F). Collectively, these findings suggest that KD causes a reduction in liver weight due to a combination of increased FA utilization and suppressed FA biosynthesis, leading to depleted hepatic FA storage.

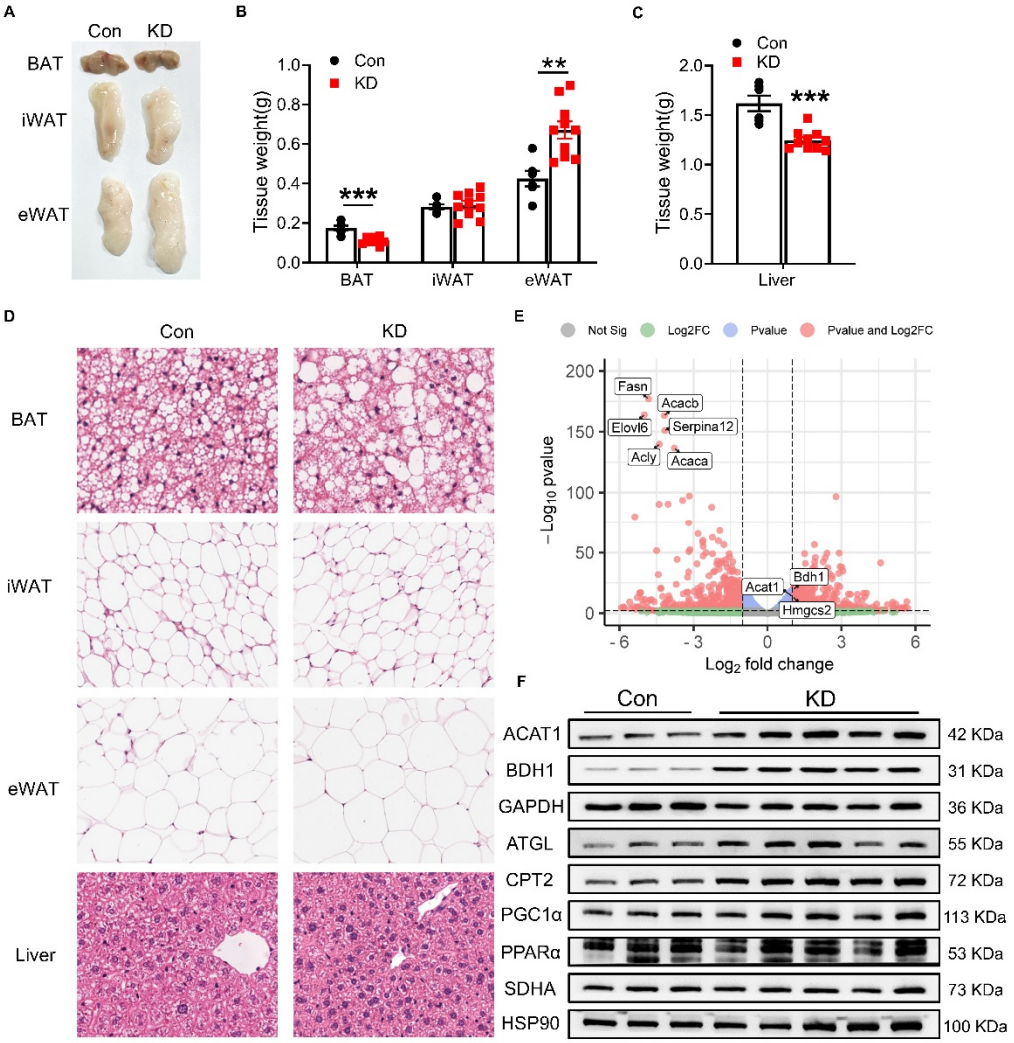

Figure 2. KD alters lipid metabolism of the mice. (A) Representative gross views of different types of adipose tissues collected from mice fed with a control diet (Con) or a ketogenic diet (KD). (B) Tissue weights of brown adipose tissue (BAT), inguinal white adipose tissue (iWAT), epididymal white adipose tissue (eWAT) and (C) Liver from mice fed with a control or a ketogenic diet. $^{**}P < 0.01$, $^{***}P < 0.001$. (D) Representative H&E staining results of BAT, iWAT, eWAT, and liver tissues from control and KD-fed mice. (E) Volcano plot showing differentially expressed genes related to lipid metabolism in liver tissues from mice fed with a control or a ketogenic diet. (F) Western blot analysis of key metabolic enzymes in liver tissues of control and KD-fed mice. Values are mean ± SEM from, n = 4-10 (B–C) individual mice per group.

3.2 KD impairs cardiac function in mice

Although DKA in T1DM is commonly marked by high blood glucose and KBs[23, 24], a nutritionally induced ketogenic state, absent the overt hyperglycemia, can also be achieved via KD. Focusing on DKA-related ketosis and the effects of a nutritionally induced ketogenic state on the heart, we assessed the cardiac function of KD-fed mice via transthoracic echocardiography. In clinics, DM patients are at higher risk of developing LV hypertrophy and often have higher resting heart rate (HR) [25, 26]. Alike that, mice fed with KD displayed an increase in the mass of LV and HR (Figures 3A-B). Similar to DM patients, mice fed with KD also have dilated atrioventricular (AV), potentially caused by the thickening of the heart walls (Figure

3C). With the above structural changes, mice within KD group, in general, have increased LVIDs (Figure 3D) and compromised ejection fraction (Figure 3E), indicating impaired cardiac function caused by impaired ketone metabolism. In addition, H&E staining indicated enlargement in the cross-section area of cardiomyocytes (Figures 3F, G).

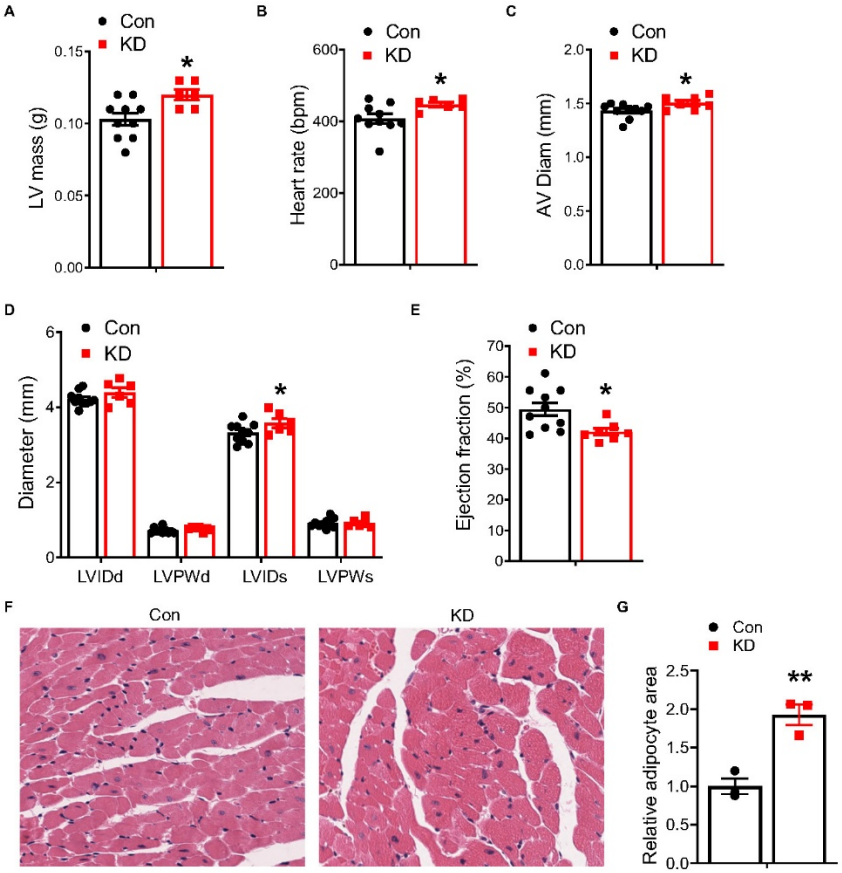

Figure 3. KD impairs cardiac function in mice. (A) Left ventricular mass (LV mass) (B) Heart rate, (C) Atrioventricular diameter (AV diameter), (D) Left ventricular internal diameter in diastole (LVIDd), systole (LVIDs), left ventricular posterior wall thickness in diastole (LVPWd), systole (LVPWs) and (E) Ejection fraction in control (Con) or ketogenic diet (KD)-fed mice. *$P < 0.05$. (F) Representative H&E staining results of cardiac tissues. (G) Quantification of adipocyte area in cardiac tissues from control (Con) or ketogenic diet (KD)-fed mice. **$P < 0.01$. Values are mean ± SEM from, n = 6-10 (A–E) or n = 3 (G) individual mice per group.

3.3 KD promotes lipid metabolic pathway and downregulates BDH1 in heart

To explore how KD affects cardiac function, we conducted RNA-sequencing analysis using LV collected from mice fed with KD or control diet and performed GO analysis on the DEGs. Clearly, the expression levels of a large group of genes related to lipid metabolic process were significantly altered by KD (Figures 4A, B). We then conducted western blotting analyses to detect levels of proteins involved in KB, glucose and FA metabolic pathways. Specifically, the protein level of ATGL, a critical enzyme that catalyzes the initial step of lipolysis, is elevated by KD (Figures 4C, D). We also found that the protein level of ACAT1 was increased, while BDH1 showed a significant decrease (Figures 4E, G). In addition, the protein level of PDHK1 has also been upregulated, favoring the metabolism of FAs over glucose (Figures 4F, G). Surprisingly, no alterations were observed in terms of mitochondrial respiratory chain enzymes (Figure 4H). These data collectively

suggest that KD significantly promotes cardiac lipid metabolic pathways and downregulates BDH1, impeding the utilization of KBs.

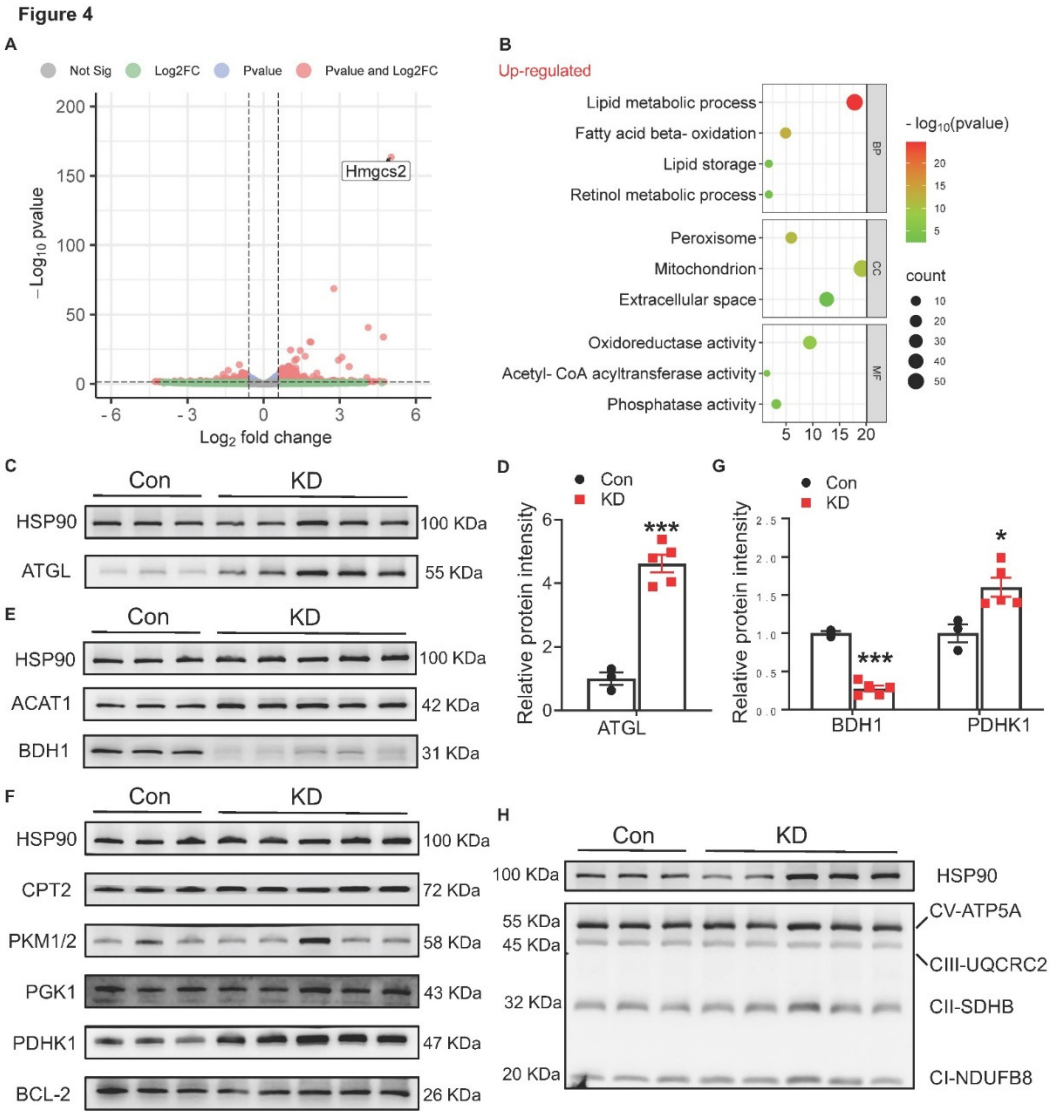

Figure 4. KD enhances cardiac lipid metabolic pathway and downregulates BDH1. (A) Volcano plot showing differentially expressed genes in cardiac tissues from control (Con) or ketogenic diet (KD)-fed mice. (F) Western blot analysis of key metabolic enzymes in cardiac tissues of control and KD-fed mice. (B) GO analysis of upregulated genes in cardiac tissues from KD-fed mice. (C-H) Western blot analysis of key metabolic enzymes in cardiac tissues from control and KD-fed mice. *$P < 0.05$, ***$P < 0.001$. Values are mean ± SEM from, n = 3-5 (D, G) individual mice per group.

3.4 Loss of Bdh1 causes cardiac dysfunction following fasting, potentially through altering histone methylation

To specifically examine the importance of BDH1 in cardiac metabolism, we generated whole-body *Bdh1* knockout mice (*Bdh1 tm1a-/-*) model and heart-specific *Bdh1* knockout mice ($Bdh1^{MKO}$). Compared to their control littermates (labeled as WT), the heart mass and heart rate of *Bdh1 tm1a-/-* mice were not changed (Figures S3A, B). While depletion of *Bdh1* induced cardiac dysfunction, showing by decreased AV diameter (Figure S3C), increased LVIDd and LVIDs (Figure S3E), as well as compromised ejection fraction (Figure S3D), these findings demonstrate a relationship between BDH1 deficiency and impaired cardiac performance. In addition to structural and functional changes, we observed no significant changes in serum AcAc or β-OHB

levels under baseline (non-fasting) conditions (Figures S3F, G), suggesting that systemic ketone levels may remain partially compensated in *Bdh1 tm1a-/-* mice in the absence of stress.

As in normal conditions, heart obtains energy from sources including glucose (20% - 40% of ATP), FFAs (40% - 60% of ATP), KBs (10% - 15% of ATP), pyruvate, and amino acids, among which KBs only contribute to a small proportion [7-11]. Thus, there was no doubt that simply knocking out *Bdh1* in the heart only mildly alter cardiac function under normal feeding scenario. (Figure 5). However, when *Bdh1*^{MKO} mice were subjected to fasting for a duration of 24 hour to induce ketogenesis [27], where the circulating level of β-OHB can by physiologically elevated and other substrates for energy production become limited, the heart starts to rely more on KBs for ATP production [28]. We found that LV mass (Figures 6A, B), LV end-diastolic volume (LVEDV), LV end-systolic volume (LVESV), and stroke volume (SV) (Figure 6C, D), as well as LVIDd and LVIDs (Figure 6E) were also significantly compromised, suggesting prominent cardiac dysfunction. Our data also showed a significant increase in serum β-OHB and a decrease in AcAc (Figure 6F, G), indicating an elevated β-OHB/AcAc ratio consistent with impaired peripheral ketone utilization.

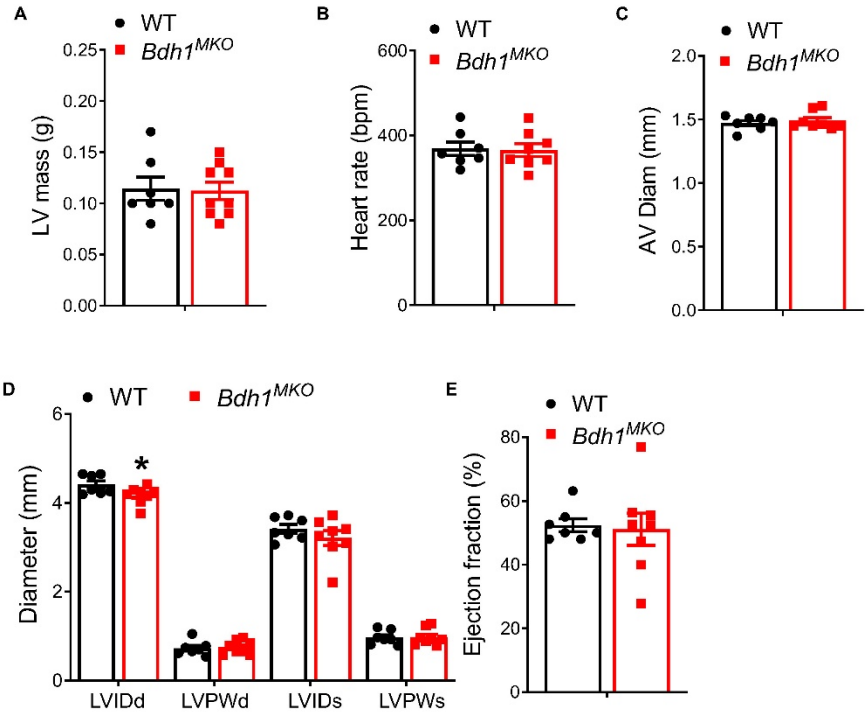

Figure 5. Heart-specific knockout of *Bdh1* mildly alter cardiac function under normal feeding scenario. (A) Left ventricular mass (LV mass), (B) Heart rate, (C) Atrioventricular diameter (AV diameter), (D) Left ventricular internal diameter in diastole (LVIDd), systole (LVIDs), left ventricular posterior wall thickness in diastole (LVPWd), systole (LVPWs) and (E) Ejection fraction in wild-type (WT) and *Bdh1*^{MKO} mice. *$P < 0.05$. Values are mean ± SEM from, n = 7-8 (A–E) individual mice per group.

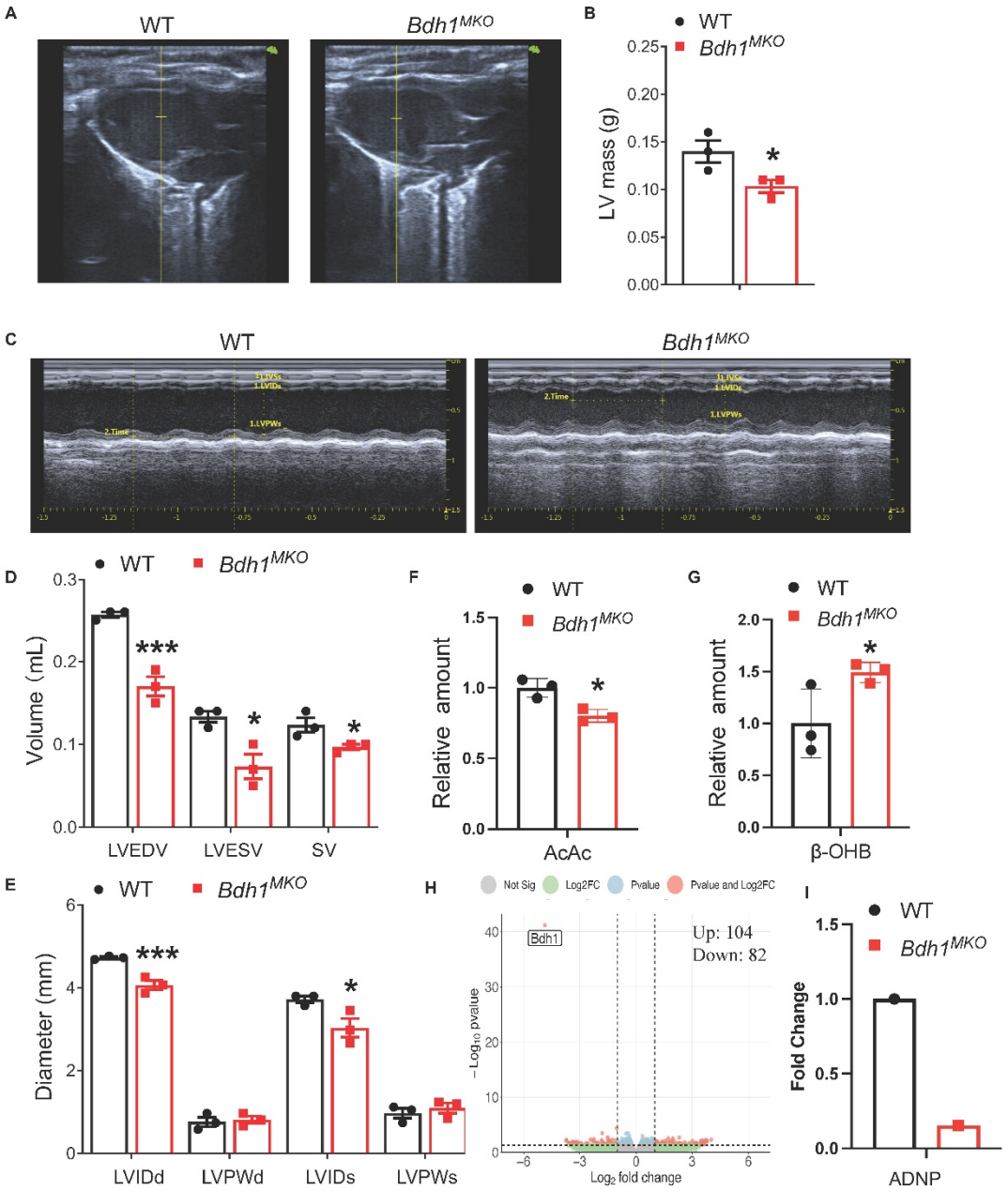

Figure 6. Heart-specific knockout of *Bdh1* causes cardiac dysfunction after 24-hour fasting. (A-C) Echocardiographic images of hearts and measurement of left ventricular mass (LV mass) in wild-type (WT) and *Bdh1*^{MKO} mice. *$P < 0.05$. (D) Measurements of left ventricular end-diastolic volume (LVEDV), left ventricular end-systolic volume (LVESV), and stroke volume (SV), (E) Left ventricular internal diameter in diastole (LVIDd), systole (LVIDs), left ventricular posterior wall thickness in diastole (LVPWd), and systole (LVPWs) in wild-type (WT) and *Bdh1*^{MKO} mice. *$P < 0.05$, ***$P < 0.001$. (F) Serum concentrations of acetoacetate (AcAc). *$P < 0.05$. (G) Serum concentrations of β-hydroxybutyrate (β-OHB). *$P < 0.05$. Values are mean ± SEM from, n = 3 (A-G) individual mice per group. (H) Volcano plot showing differentially expressed genes in cardiac tissues from wild-type (WT) and *Bdh1*^{MKO} mice. (I) Relative mRNA expression level of ADNP in cardiac tissues from wild-type (WT) and heart-specific Bdh1 knockout (Bdh1MKO) mice under fasting condition. Data are shown as fold change normalized to WT.

To further evaluate the potential molecular and metabolic alterations with *Bdh1*-deficient heart, we conducted western blotting analyses to evaluate the expression levels of key proteins involved in KB, glucose and FA metabolic pathways. BDH1 was found to be completely deleted in the heart of global and conditional *Bdh1* knockout mice (Figures 7A, B), showing the success of model construction. However, In both global and cardiac-specific Bdh1 knockout mice, the protein levels of ACAT1, as well as proteins involved in glucose and FA metabolism, remained unchanged (Figures 7A, B). Recent studies have demonstrated that in

addition to serving as an alternative energy source, β-OHB can augment overall histone acetylation and histone methylation levels in cells [29, 30]. Therefore, we analyzed the acetylation and methylation levels of H3K27 in the heart tissues. Notably, depletion of *Bdh1* significantly reduced the level of H3K27ME (Figures 7C, D). Taken together, these results indicate that loss of *Bdh1* causes cardiac dysfunction and disrupts histone methylation.

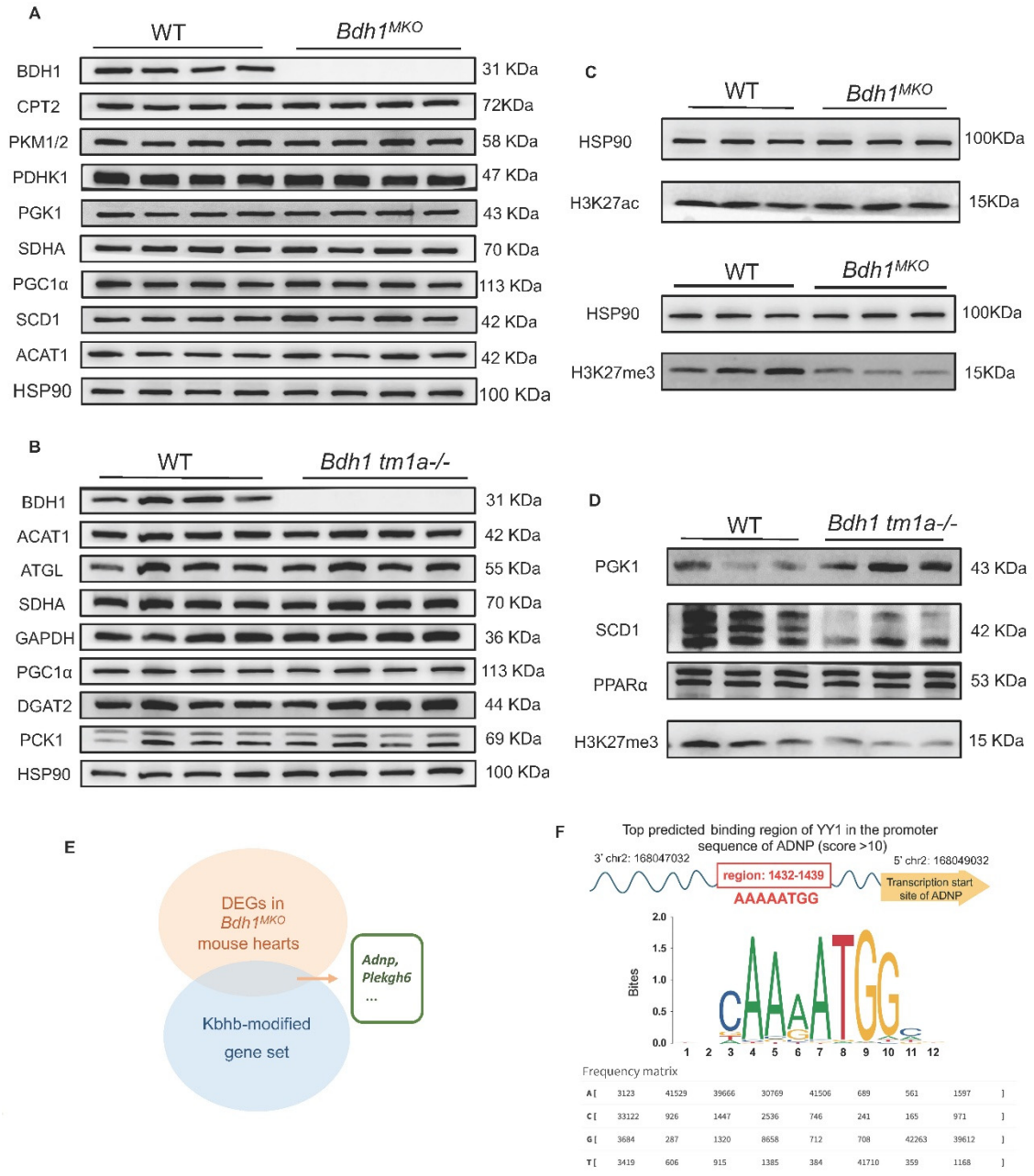

Figure 7. Heart-specific knockout of *Bdh1* affects histone methylation. (A-D) Western blot analysis of key metabolic enzymes and histone modification markers in cardiac tissues from wild-type (WT) and *Bdh1* knockout mice (*Bdh1*^{MKO} and *Bdh1 tm1a-/-*). (E) Overlap between differentially expressed genes in *Bdh1*^{MKO} mice hearts and Kbhb-modified gene set. Shared genes such as Adnp and Plekhg6 were identified as candidates (F) Predicted YY1 binding motifs within the ADNP promoter region.

To further identify potential epigenetic regulatory targets downstream of BDH1 deficiency, we compared our RNA-seq dataset with a published β-hydroxybutyrylation (Kbhb)-modified gene set [31, 32]. Among the overlapping genes, ADNP and PLEKHG6 emerged as promising candidates due to their functional relevance

to cardiac development and remodeling. Notably, ADNP is a chromatin regulatory factor whose mutations are implicated in Helsmoortel–Van der Aa syndrome, with congenital heart defects observed in up to 38% of affected individuals[33]. Likewise, PLEKHG6 (also known as MyoGEF) is a RhoA-related guanine nucleotide exchange factor with well-established roles in cytoskeletal dynamics, and its suppression may disrupt actomyosin architecture critical for myocardial contractile integrity[34, 35].

Motif analysis of their promoter regions using the JASPAR 2024 database revealed high-confidence binding sites for YY1 and E2F6, two transcription factors known to recruit Polycomb complexes and mediate transcriptional repression (Figures 7E, F)[36, 37]. These data suggest that transcriptional suppression of these genes may result from epigenetic silencing mechanisms that are modulated by BDH1-dependent βOHB-Kbhb signaling. This epigenetic dysregulation may contribute to the impaired myocardial function observed in BDH1-deficient models.

3.5 Diabetic conditions alter FA and KB metabolisms of the heart

To systematically characterize how ketone body metabolism is altered across different diabetic models, we firstly conducted proteomic analysis of LV tissues from STZ-induced T1DM mice and RNA-sequencing analysis of *db/db* transgenic T2DM mice, along with their respective control littermates. Throughout the progression of T1DM development (1-, 2-, 3-, and 4-months post STZ injection), we observed an upregulation of proteins associated with KB metabolism (OXCT1, BDH1, HMGCL, and ACAT1) and a decrease in the expression of FASN, a protein involved in fatty acid synthesis (Figure 8A). Notably, at 4 months post STZ injection, all samples exhibited high expression levels of BDH1. β-OHB shows an altered ratio of β-OHB to AcAc, which can increase from 1:1-3:1 to 10:1 in diabetic patients[24]. In STZ-induced T1DM mice, blood β-OHB concentration progressively rises with diabetic progression, while the level of palmitic acid, a common saturated fatty acid, declines over time (Figure 8C, D), with a significant reduction of AcAc in the serum of T1DM mice (Figure 8E), thereby confirming an altered β-OHB/AcAc ratio under hyperketonemic conditions. These findings indicate that STZ-induced T1DM conditions influence the availability of FAs and KBs for cardiac metabolism, potentially leading to a shift in the heart's preferred fuel source from FFAs to KBs.

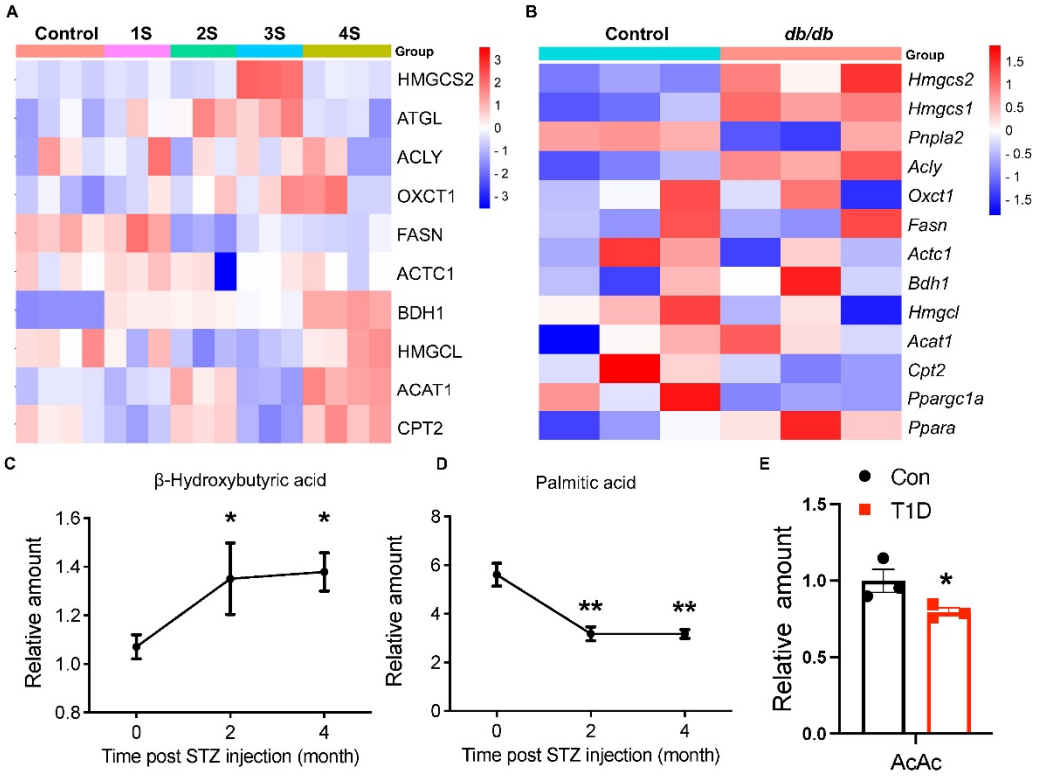

Figure 8. Altered lipid and ketone metabolic pathways from heart of diabetes mice. (A) Heatmap of the differentially expressed proteins associated with fatty acid and ketone body metabolism in the LV tissues of STZ-induced T1DM mice at 1-, 2-, 3-, and 4-months post-injection relative to control mice. The data were derived from a proteomic analysis. (B) Differential gene expression in the LV of *db/db* transgenic T2DM mice and control littermates highlighted through RNA sequencing. (C-D) Time-course profiling of β-hydroxybutyrate and palmitic acid in serum from STZ-induced T1DM mice, assessed by untargeted metabolomics. $*P < 0.05$, $**P < 0.01$ vs. 0-month time point. (E) Serum concentrations of acetoacetate (AcAc) from STZ-induced T1DM (T1D) mice, assessed by targeted quantification. $*P < 0.05$. Values are mean ± SEM from, n = 3 (C-E) individual mice per group.

We also profiled the cardiac gene expression patterns of control and the genetic T2DM *db/db* mice. gene ontology (GO) analysis revealed that differential expressed genes (DEGs) that were upregulated in *db/db* mice enriched in extracellular, proteolysis, endoplasmic reticulum and cytoskeleton, etc. (Figure S4A). While the downregulated DEGs were enriched in metabolism and muscle contractions (Figure S4B). Intriguingly, hearts collected from *db/db* mice exhibited upregulation of key genes involved in both ketogenesis and FA biosynthesis (*Hmgcs2*, *Hmgcs1*, and *Acly*) (Figure 8B). However, no significant changes were noted in the expression levels of key enzymes in the KB oxidation pathway. To validate the observed alterations in cardiac FA and KB metabolism in T2DM mice, we administered a HFD to adult wildtype mice, followed by low-dose of STZ injection to induce conditions mimicking T2DM. Consistent with the initial manifestation of diabetic cardiomyopathy as isolated diastolic dysfunction in T2DM patients[25, 38], our T2DM mice displayed a decrease in left ventricular mass (LV mass), heart rate, aortic valve diameter (AV diam) and left ventricular internal diameter in diastole (LVIDd), indicative of potential cardiac hypertrophy (Figures 9A-D). Notably, no significant changes were observed in left ventricular internal diameter in systole (LVIDs) or left ventricular posterior wall thickness (LVPWs) (Figure 9D). Additionally, these T2DM mice exhibited a reduced ejection fraction rate, suggesting the presence of cardiomyopathy (Figure 9E). Similar to the findings in STZ-induced T1DM, alterations in the cardiac protein levels of key enzymes involved in metabolic pathways were evident

in T2DM mice. Specifically, T2DM conditions suppressed the protein level of BDH1 and markedly elevated the levels of PDHK1 and PPARα (Figure 9F), indicating a metabolic shift from glucose oxidation to fatty acid oxidation, reflecting an adaptive response favoring FFAs over both KBs and glucose. Consistent with these findings, T2DM mice also exhibited significant elevations in circulating β-OHB, whereas AcAc remained unchanged, as revealed by targeted serum assays (Figure 9G, H).

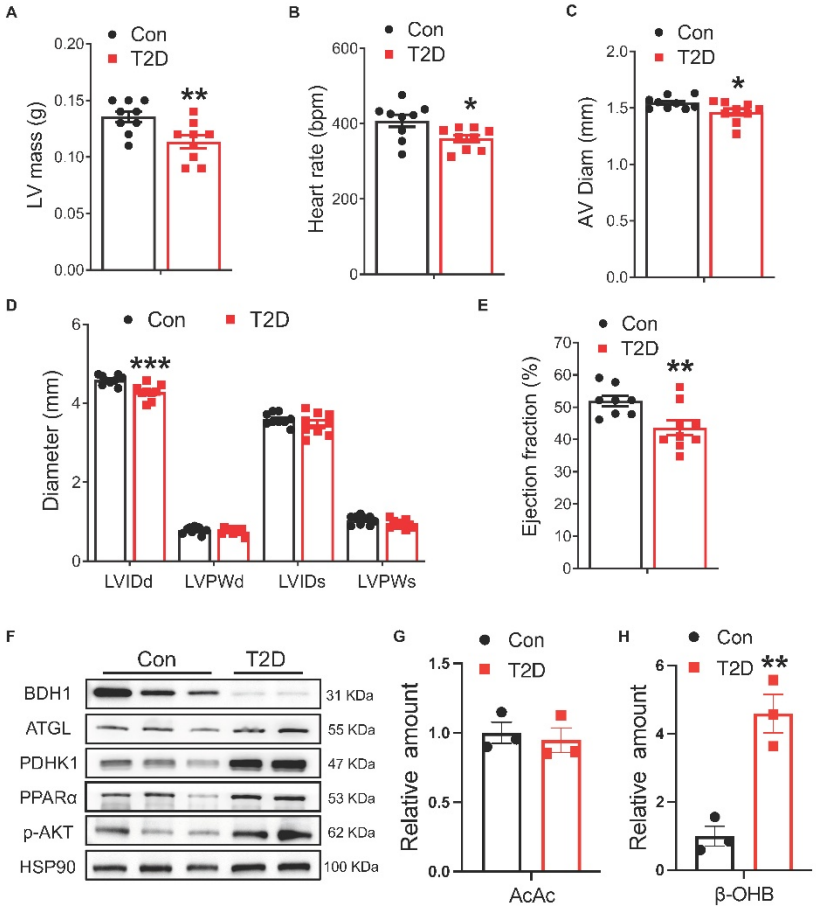

Figure 9. Impaired cardiac function of T2D mice and altered lipid and ketone metabolic pathways in heart. (A) Left ventricular mass (LV mass), (B) Heart rate, (C) Atrioventricular diameter (AV diameter), (D) Left ventricular internal diameter in diastole (LVIDd), systole (LVIDs), left ventricular posterior wall thickness in diastole (LVPWd), systole (LVPWs) and (E) Ejection fraction in control (Con) and HFD+STZ-induced T2DM (T2D) mice. *$P < 0.05$, **$P < 0.01$, ***$P < 0.001$. (F) Western blot analysis of key metabolic enzymes in LV tissues of control and T2D mice. (G) Serum concentrations of acetoacetate (AcAc). (G) Serum concentrations of β-hydroxybutyrate (β-OHB). **$P < 0.01$. Values are mean ± SEM from, n = 8-9 (A-E) or n = 3 (G-H) individual mice per group.

Collectively, our findings suggest that the hearts of both T1DM and T2DM mice exhibit significant alterations in FFA and KB metabolism. Notably, the observed changes in key enzyme BDH1 underscore its potential role as a critical mediator in both diabetic conditions (Figures 8A, 9F).

4. Discussion

KD can confer wide-ranging health benefits, including weight loss, decreased inflammation, enhanced brain function, and protection against cancer.[1, 3-5] Despite these advantages, its long-term cardiac effects remain a matter of debate, as increasing evidence suggests that myocardial adaptations to KD are highly context-dependent.[6] Indeed, while some studies show potential cardioprotective properties of KD against ischemia/reperfusion injury, hypertension [6, 39], others report that KD might induce adverse outcomes such as

fibrosis or diminished cardiac function under certain conditions.[40] Of particular note, many KD or high-fat diet interventions demonstrating weight-loss benefits do not compare outcomes to standard chow conditions, leaving the true impact on normal dietary backgrounds less clear.

One of the main ways KD may affect the heart is by markedly elevating circulating KBs, especially β-OHB. Although the failing heart seems to upregulate KB utilization as an alternative fuel.[41] , chronically elevated KBs have also been linked to disease severity in heart failure.[22, 41] This ambiguity likely reflects the complexity of metabolic interactions in the heart, where glucose, FFAs, and KBs all vie to fuel myocardial ATP production.[7-11]

This study demonstrates that KD intervention alters cardiac BDH1 expression, inducing a cardiomyopathy-like phenotype. Specifically, our nutritional intervention model reveals that chronic KD exposure downregulates BDH1, resulting in a paradoxical impairment of myocardial ketone utilization despite systemic ketosis. Notably, this discrepancy between high circulating ketones and diminished myocardial ketolysis may contribute to adverse cardiac outcomes under prolonged ketogenic conditions. Similar concerns have been raised by Sternberg et al., who demonstrated that both LCT-based and mixed LCT/MCT KD induced cardiac fibrosis in healthy mice[42]. Their findings suggest that high-fat-driven ketosis may impose cardiac stress regardless of MCT inclusion. Importantly, the KD formulation used in our study (Cat#D10070801) is also rich in long-chain fatty acids (cocoa butter, soybean oil), aligning with the lipid profile in Sternberg's model. This similarity supports the relevance of our observations and highlights the need to consider both dietary fat composition and myocardial ketone utilization capacity when evaluating the cardiac safety of KD. Subsequently, we generated *Bdh1 tm1a-/-* and *Bdh1*^{MKO} mice to elucidate the potential role of BDH1 in regulating cardiac function. We then used STZ-induced T1DM mice, transgenic *db/db* mice, and HF+STZ-induced T2DM mice to study changes in KB metabolism and Bdh1 expression under diabetic conditions. Our findings indicate that KD impairs BDH1-dependent ketone oxidation, leading to cardiac structural remodeling, disrupted lipid metabolism, and reduced contractile performance. Moreover, BDH1 appears to play a critical role in the development of HF under diabetic conditions by modulating histone methylation.

Notably, in addition to the inconsistency of BDH1 expression in the hearts of mice with varying diabetic models, we also observed divergence in echocardiography phenotypes between the global and heart-specific *Bdh1* knockout mice. *Bdh1 tm1a-/-* animals exhibited systolic dysfunction under normal conditions yet maintained normal circulating β-OHB and AcAc. By contrast, *Bdh1*^{MKO} mice remained haemodynamically normal when fed but, after a 24-h fast, developed cardiac dysfunction. *Bdh1*^{MKO} eliminates BDH1 only in the heart. Hepatic ketone production therefore remains intact, but cardiac β-OHB oxidation is curtailed. Under normal conditions, the myocardium derives 40–60 % of ATP from FFAs and only -10 % from ketones[7-11]. And KBs act as a major alternative energy source for the heart when other substrates are scarce, such as during prolonged fasting[43].These factors could potentially explain why an evident phenotype under normal conditions was only observable in *Bdh1 tm1a-/-* mice, and why cardiac dysfunction in *Bdh1*^{MKO} mice was

detected only post-fasting. To further investigate the metabolic basis, we assessed key enzymes involved in ketone, lipid, and glucose metabolism by Western blotting, revealing that KD-induced remodeling was attenuated in BDH1-deficient hearts.

Serum analyses add a systemic dimension to these tissue specific effects. After a 24h fasting, *Bdh1*^{MKO} mice demonstrated β-OHB elevation with concomitant AcAc reduction, yielding a higher β-OHB/AcAc ratio. The same qualitative pattern was observed in T1DM and T2DM models. Conversely, a research reported that fasting challenged *Bdh1 tm1a-/-* mice showed the opposite shift, with lower β-OHB and higher AcAc levels[44], consistent with impaired hepatic ketogenesis. Similar context-dependent behaviours have been reported elsewhere: muscle-specific BDH1 deletion increases β-OHB only after fasting[45], whereas hepatocyte-BDH1 loss suppresses β-OHB and raises AcAc[46]. Together, these data indicate that the direction of circulating ketone change is dictated by the principal site of BDH1 perturbation and by metabolic context (e.g, fed, fasted, diabetic), rather than pointing to a single rate-limiting step. In T1DM, the parallel rise of β-OHB and myocardial BDH1 may reflect a compensatory attempt to enhance β-OHB clearance, although alternative mechanisms such as altered hepatic redox equilibrium, renal re-uptake, or extra-hepatic oxidation cannot be excluded. Future isotope-tracing and tissue specific rescue experiments will be required to define how BDH1 orchestrates systemic cardiac ketone flux under physiological and pathophysiological ketosis.

In investigating the mechanisms through which BDH1 deficiency influences cardiac function, we assessed its effect on histone acetylation and methylation. Considering that β-OHB, an endogenous histone deacetylase (HDAC) inhibitor, has been shown to augment histone acetylation in certain cell types [29], BDH1 depletion could potentially alter β-OHB levels, and consequently, histone acetylation in the heart. Western blotting analysis, however, did not reveal significant alterations in H3K27AC levels in LV tissues from either *Bdh1 tm1a-/-* or *Bdh1*^{MKO} mice when compared to those from their genetically unmodified littermates. Surprisingly, both groups displayed reductions in H3K27ME, with comparable extents of reduction observed in LV tissues of *Bdh1 tm1a-/-* and *Bdh1*^{MKO} mice. This observation implies that the decrease in histone methylation might be directly attributable to BDH1 deficiency, rather than its indirect impacts, such as through altering circulating β-OHB levels. These findings strongly advocate for further research into BDH1's potential role in modulating histone methylation.

Consistent with this, ADNP and PLEKHG6 were identified as genes of interest through cross-referencing our RNA-seq data with a published Kbhb-modified gene set. Motif analysis of their promoter regions using the JASPAR 2024 database revealed high-confidence binding sites for YY1 and E2F6, two transcription factors known to facilitate Polycomb complex recruitment. Specifically, YY1 can directly interact with the canonical PRC2 complex to promote H3K27me3 deposition, whereas E2F6 is a core DNA-binding component of the non-canonical PRC1.6 complex that mediates H2AK119ub1 and subsequently enhances PRC2 recruitment[36, 37].

The observed downregulation of H3K27me3 in BDH1-deficient hearts, along with the identification of Polycomb-associated motifs in ADNP and PLEKHG6 promoters, suggests potential disruption of chromatin

repression pathways due to altered β-OHB-Kbhb signaling. While β-OHB was not directly measured in cardiac tissue, BDH1-dependent local metabolic flux may influence chromatin accessibility or transcription factor interactions, thereby disrupting normal Polycomb recruitment and histone methylation. Given the established role of ADNP in cardiac development and of PLEKHG6 in cytoskeletal regulation and RhoA signaling[34, 35], this epigenetic dysregulation may contribute to the myocardial dysfunction observed in BDH1-deficient models.

KBs, predominantly produced by the liver, act as an alternate energy source in peripheral tissues when glucose supply is suboptimal [13, 16, 47, 48]. Pathological rises in blood KB levels are primarily associated to DM [24, 49]. In the population of individuals with DM, some develop a condition known as diabetic cardiomyopathy, which is characterized by myocardial dysfunction in the absence of coronary artery disease, valvular disease, or other cardiac risk factors [25]. Despite the term being introduced in 1972 [50], the precise etiology and underlying mechanisms of HF in DM patients remain largely elusive, particularly regarding the role of KB metabolism in its pathological progression.

KB metabolism comprises ketogenesis and ketolysis, processes that facilitate the transformation of FFA-derived resources into KBs within the liver, which are then metabolized by other tissues [16]. Predominantly, the heart, reputed as a major consumer of KBs [28], relies on this energy source during periods of restricted availability of alternative substrates [51]. Under physiological conditions, insulin serves a regulatory role by inhibiting ketogenesis through the dephosphorylation of hormone-sensitive lipase, as well as by catalyzing lipogenesis via the stimulation of acetyl-CoA carboxylase [13, 16]. Consequently, the dephosphorylation of hormone-sensitive lipase in adipocytes impedes the conversion of triglycerides to FA and glycerol, constraining the release of FFAs, and thus mitigating the substrate supply for hepatic ketogenesis [16]. However, DKA, characterized by enhanced ketogenesis owing to diminished insulin levels and escalated counterregulatory hormones, results in a pathological elevation in circulating KBs[24]. In this study, the replication of T1DM conditions via STZ administration to sabotage β-cell, thereby curbing insulin production that sequentially released the inhibitory impact on hepatic ketogenesis, led to a notable rise in circulating β-OHB levels. Correspondingly, an observed upregulation in the heart's BDH1 protein level, a crucial component in the KB oxidation pathway, heightens KB utilization through β oxidation. However, in an effort to exclusively emulate the elevation in circulating β-OHB in STZ-induced T1DM mice while simultaneously circumventing potential interference with other metabolic aspects, a KD was given to adult male mice. This resulted in noticeable differences in the heart's KB metabolism as compared to STZ-induced T1DM mice, specifically in the diminished cardiac BDH1 levels, akin to our T2DM model induced by a HFD and low dosage of STZ. The KD, comprising high-fat constituents such as soybean oil or cocoa butter with minimal carbohydrates and adequate protein, not only stimulates hepatic ketogenesis but also introduces redundant FFAs, the heart's preferred energy substrate. Consequently, the heart predominantly utilizes FFAs for energy, thereby inhibiting its capacity to transition from FFAs to KBs or glucose, a phenomenon referred to as

metabolic inflexibility[2]. Hence, the observed decrease in the heart's BDH1 protein level indicates a reduction in KD β oxidation.

From a translational perspective, our findings raise important considerations for the clinical use of KD, particularly in individuals with diabetes or compromised myocardial metabolic flexibility. Although KD has shown short-term benefits for glycemic control and weight reduction, our study suggests that its long-term application may pose risks to cardiac health in contexts where BDH1-dependent ketone oxidation is impaired. In diabetic cardiomyopathy, a condition marked by metabolic inflexibility and elevated systemic ketones, downregulation of myocardial BDH1 could exacerbate energetic imbalance and epigenetic disruption, leading to contractile dysfunction. These insights highlight the importance of evaluating both systemic ketone levels and cardiac ketolytic capacity in patients undergoing dietary ketosis. Future interventions aimed at preserving or restoring BDH1 expression may offer novel therapeutic opportunities to improve cardiac resilience in metabolic disorders. While our study identifies a clear association between BDH1 deficiency and myocardial dysfunction, further studies incorporating gain-of-function approaches (e.g., BDH1 overexpression or reconstitution) are warranted to assess the reversibility and therapeutic potential of restoring BDH1 expression. Moreover, although the current work focused on early stage adaptation to ketogenic challenge, the long-term cardiac effects of sustained KD remain an important area for future research.

5. Conclusions

This study focuses on the impact of KD on cardiac function and metabolic pathways. We found that although KD markedly promotes lipid utilization and KB synthesis at the systemic level, it significantly downregulates BDH1 in the heart, thereby inhibiting effective utilization of KBs (especially β-OHB). This results in "impaired KB oxidation" and cardiac structural remodeling, accompanied by dysregulated lipid metabolism and compromised contractile function. Results suggest that alterations in histone methylation could be a potential underlying mechanism. In various diabetic mouse models that mimic diabetic conditions demonstrated that diabetes also altered *Bdh1* expression and the cardiac fuel source. These findings indicate that KD does not necessarily confer cardiac protection under all metabolic conditions, despite its benefits in glycemic control for some metabolic disorders (e.g., T2DM), it may pose cardiac risks if BDH1 is impaired or suppressed. Future research efforts could focus on the modulation of BDH1 activity, the improvement of cardiac metabolic flexibility, and the elucidation of epigenetic mechanisms, thereby providing new insights and refined strategies for the safe clinical application of KD and the comprehensive management of diabetes and other metabolic diseases.

Ethics Approval and Consent to Participate

All procedures involving animals were carried out following the ethical standards and guidelines for animal care established by Institutional Animal Care and Use Committee of CAM-SU. The research protocols used in this study were approved by institutional Animal Care and Use Committee of CAM-SU on December 24th, 2021.

Consent for Publication

Not applicable (no personal data is being published).

Data Availability

The data supporting this article have been included as part of the Supplementary Information.

Competing Interests

The authors declare no competing interests.

Funding

This work was partially supported by National Natural Science Foundation of China (82070838 to Yu Feng, 32100944 to Zhihao Jia and 82270755 to Hong Sun), SIP High-Quality Innovation Platform for Chronic Diseases (YZCXPT2022203), Natural Science Foundation of Jiangsu Province (BK20210715 to Zhihao Jia), Gusu Innovation and Entrepreneur Leading Talents project (ZXL2023200 to Zhihao Jia), and Ministry of Science and Technology (2018YFA0801102 to Yingying Dong).

Acknowledgement

We acknowledge Figdraw for their assistance in creating the Graphical Abstract.

References

[1] K. Dowis, S. Banga, The Potential Health Benefits of the Ketogenic Diet: A Narrative Review, Nutrients. 13 (2021) 1654. https://doi.org/10.3390/nu13051654.

[2] R.H. Eckel, K.E. Bornfeldt, I.J. Goldberg, Cardiovascular disease in diabetes, beyond glucose, Cell Metab. 33 (2021) 1519-1545. https://doi.org/10.1016/j.cmet.2021.07.001.

[3] K.W. Lange, J. Guo, S. Kanaya, et al., Medical foods in Alzheimer's disease, Food Sci. Hum. Wellness. 8 (2019) 1-7. https://doi.org/10.1016/j.fshw.2019.02.002.

[4] K.W. Lange, Y. Nakamura, N. Chen, et al., Diet and medical foods in Parkinson's disease, Food Sci. Hum. Wellness. 8 (2019) 83-95. https://doi.org/10.1016/j.fshw.2019.03.006.

[5] D.D. Weber, S. Aminzadeh-Gohari, J. Tulipan, et al., Ketogenic diet in the treatment of cancer - Where do we stand?, Mol. Metab. 33 (2020) 102-121. https://doi.org/10.3390/nu13051654.

[6] S. Takahara, S. Soni, Z.H. Maayah, et al., Ketone therapy for heart failure: current evidence for clinical use, Cardiovascular Research. 118 (2022) 977-987. https://doi.org/10.1093/cvr/cvab068.

[7] G.D. Lopaschuk, J.R. Ussher, C.D. Folmes, et al., Myocardial fatty acid metabolism in health and disease, Physiol Reviews. 90 (2010) 207-258. https://doi.org/10.1152/physrev.00015.2009.

[8] G.W. Goodwin, C.S. Taylor, H. Taegtmeyer, Regulation of energy metabolism of the heart during acute increase in heart work, The Journal of Biological Chemistry. 273 (1998) 29530-29539. https://doi.org/10.1074/jbc.273.45.29530.

[9] G.D. Lopaschuk, Q.G. Karwi, R. Tian, et al., Cardiac Energy Metabolism in Heart Failure, Circ Res. 128 (2021) 1487-1513. https://doi.org/10.1161/CIRCRESAHA.121.318241.

[10] M.D. Neinast, C. Jang, S. Hui, et al., Quantitative Analysis of the Whole-Body Metabolic Fate of Branched-Chain Amino Acids, Cell Metabablism. 29 (2019) 417-429. https://doi.org/10.1016/j.cmet.2018.10.013.

[11] A.A. Gibb, B.G. Hill, Metabolic Coordination of Physiological and Pathological Cardiac Remodeling, Circ. Res. 123 (2018) 107-128. https://doi.org/10.1161/CIRCRESAHA.118.312017.

[12] M. Pawlak, E. Bauge, F. Lalloyer, et al., Ketone Body Therapy Protects From Lipotoxicity and Acute Liver Failure Upon Pparalpha Deficiency, Mol Endocrinol. 29 (2015) 1134-1143. https://doi.org/10.1210/me.2014-1383.

[13] S.R. Yurista, C.T. Nguyen, A. Rosenzweig, et al., Ketone bodies for the failing heart: fuels that can fix the engine?, Trends Endocrinol Metab. 32 (2021) 814-826. https://doi.org/10.1016/j.tem.2021.07.006.

[14] T.R. Matsuura, P. Puchalska, P.A. Crawford, et al., Ketones and the Heart: Metabolic Principles and Therapeutic Implications, Circ Res. 132 (2023) 882-898. https://doi.org/10.1161/CIRCRESAHA.123.321872.

[15] G. Aubert, O.J. Martin, J.L. Horton, et al., The Failing Heart Relies on Ketone Bodies as a Fuel, Circulation. 133 (2016) 698-705. https://doi.org/10.1161/CIRCULATIONAHA.115.017355.

[16] P. Puchalska, P.A. Crawford, Multi-dimensional Roles of Ketone Bodies in Fuel Metabolism, Signaling, and Therapeutics, Cell Metab. 25 (2017) 262-284. https://doi.org/10.1016/j.cmet.2016.12.022.

[17]G.F. Cahill Jr, R.L. Veech, Ketoacids? Good medicine?, Transactions of the American Clinical and Climatological Association. 114 (2003) 149-161.

[18] Y. Li, Q. Liu, Z. Jia, et al., Ketone bodies in exercise, health and disease: Metabolic mechanisms, pathophysiology, and therapeutic implications, Advanced Exercise and Health Science. 2 (2025) 83-93. https://doi.org/10.1016/j.aehs.2025.05.004.

[19] A.L. Lehninger, H.C. Sudduth, J.B. Wise, D-beta-Hydroxybutyric dehydrogenase of muitochondria, J Biol Chem. 235 (1960) 2450-2455. https://www.ncbi.nlm.nih.gov/pubmed/14415394

[20] T. Yokokawa, Y. Sugano, A. Shimouchi, et al., Exhaled Acetone Concentration Is Related to Hemodynamic Severity in Patients With Non-Ischemic Chronic Heart Failure, Circ J. 80 (2016) 1178-1186. https://doi.org/10.1253/circj.CJ-16-0011.

[21] J.H. Chung, J.S. Kim, O.Y. Kim, et al., Urinary ketone is associated with the heart failure severity, Clin Biochem. 45 (2012) 1697-1699. https://doi.org/10.1016/j.clinbiochem.2012.08.013.

[22] J.-P. Song, L. Chen, X. Chen, et al., Elevated plasma β-hydroxybutyrate predicts adverse outcomes and disease progression in patients with arrhythmogenic cardiomyopathy, Sci. Transl. Med. 12 (2020) 8329. https://doi.org/10.1126/scitranslmed.aay8329.

[23] P. Felig, Diabetic ketoacidosis, N Engl J Med. 290 (1974) 1360-1363. https://doi.org/10.1056/NEJM197406132902405.

[24] L. Laffel, Ketone bodies: a review of physiology, pathophysiology and application of monitoring to diabetes, Diabetes/Metabolism Research and Reviews. 15 (1999) 412-426. https://doi.org/10.1002/(SICI)1520-7560(199911/12)15:6<412::AID-DMRR72>3.0.CO;2-8.

[25] Y. Tan, Z. Zhang, C. Zheng, et al., Mechanisms of diabetic cardiomyopathy and potential therapeutic strategies: preclinical and clinical evidence, Nat Rev Cardiol. 17 (2020) 585-607. https://doi.org/10.1038/s41569-020-0339-2.

[26] M. Lehrke, N. Marx, Diabetes Mellitus and Heart Failure, Am J Cardiol. 120 (2017) S37-S47. https://doi.org/10.1016/j.amjcard.2017.05.014.

[27] G.F. Cahill, Jr., Fuel metabolism in starvation, Annu Rev Nutr. 26 (2006) 1-22. https://doi.org/10.1146/annurev.nutr.26.061505.111258.

[28] D.G. Cotter, R.C. Schugar, P.A. Crawford, Ketone body metabolism and cardiovascular disease, Am J Physiol Heart Circ Physiol. 304 (2013) H1060-1076. https://doi.org/10.1152/ajpheart.00646.2012.

[29] T. Shimazu, M.D. Hirschey, J. Newman, et al., Suppression of oxidative stress by beta-hydroxybutyrate, an endogenous histone deacetylase inhibitor, Science. 339 (2013) 211-214. https://doi.org/10.1126/science.1227166.

[30] Y. Chu, C. Zhang, M. Xie, Beta-Hydroxybutyrate, Friend or Foe for Stressed Hearts, Front Aging. 2 (2021) https://doi.org/10.3389/fragi.2021.681513.

[31] Z. Xie, D. Zhang, D. Chung, et al., Metabolic Regulation of Gene Expression by Histone Lysine β-Hydroxybutyrylation, Mol. Cell. 62 (2016) 194-206. https://doi.org/10.1016/j.molcel.2016.03.036.

[32] M. Tang, Y. Tu, Y. Gong, et al., β-hydroxybutyrate facilitates mitochondrial-derived vesicle biogenesis and improves mitochondrial functions, Mol. Cell. 85 (2025) 1395-1410. https://doi.org/10.1016/j.molcel.2025.02.022.

[33] A. Van Dijck, A.T. Vulto-van Silfhout, E. Cappuyns, et al., Clinical Presentation of a Complex Neurodevelopmental Disorder Caused by Mutations in ADNP, Biol. Psychiatry. 85 (2019) 287-297. https://doi.org/10.1016/j.biopsych.2018.02.1173.

[34] R. D'Angelo, S. Aresta, A. Blangy, et al., Interaction of ezrin with the novel guanine nucleotide exchange factor PLEKHG6 promotes RhoG-dependent apical cytoskeleton rearrangements in epithelial cells, Mol. Biol. Cell. 18 (2007) 4780-4793. https://doi.org/10.1091/mbc.e06-12-1144.

[35] D. Wu, M. Asiedu, Q. Wei, Myosin-interacting guanine exchange factor (MyoGEF) regulates the invasion activity of MDA-MB-231 breast cancer cells through activation of RhoA and RhoC, Oncogene. 28 (2009) 2219-2230. https://doi.org/10.1038/onc.2009.96.

[36] E.M. Mendenhall, R.P. Koche, T. Truong, et al., GC-Rich Sequence Elements Recruit PRC2 in Mammalian ES Cells, PLos Genet. 6 (2010) e1001244. https://doi.org/10.1371/journal.pgen.1001244.

[37] B. Stielow, F. Finkernagel, T. Stiewe, et al., MGA, L3MBTL2 and E2F6 determine genomic binding of the non-canonical Polycomb repressive complex PRC1.6, PLos Genet. 14 (2018) e1007193. https://doi.org/10.1371/journal.pgen.1007193.

[38] P.M. Seferovic, W.J. Paulus, Clinical diabetic cardiomyopathy: a two-faced disease with restrictive and dilated phenotypes, Eur. Heart J. 36 (2015) 1718-1727. https://doi.org/10.1093/eurheartj/ehv134.

[39] Y. Guo, C. Zhang, F.-F. Shang, et al., Ketogenic Diet Ameliorates Cardiac Dysfunction via Balancing Mitochondrial Dynamics and Inhibiting Apoptosis in Type 2 Diabetic Mice, Aging and Disease. 11 (2020) 229-240. https://doi.org/10.14336/ad.2019.0510.

[40] S. Xu, H. Tao, W. Cao, et al., Ketogenic diets inhibit mitochondrial biogenesis and induce cardiac fibrosis, Signal Transduction Targeted Ther. 6 (2021) 54. https://doi.org/10.1038/s41392-020-00411-4.

[41] D. Murashige, C. Jang, M. Neinast, et al., Comprehensive quantification of fuel use by the failing and nonfailing human heart, Science. 370 (2020) 364-368. https://doi.org/10.1126/science.abc8861.

[42] F. Sternberg, C. Sternberg, A. Dunkel, et al., Ketogenic diets composed of long-chain and medium-chain fatty acids induce cardiac fibrosis in mice, Mol. Metab. 72 (2023) 101711. https://doi.org/10.1016/j.molmet.2023.101711.

[43] A. Abdul Kadir, K. Clarke, R.D. Evans, Cardiac ketone body metabolism, Biochim Biophys Acta Mol Basis Dis. 1866 (2020) 165739. https://doi.org/10.1016/j.bbadis.2020.165739.

[44] H. Otsuka, T. Kimura, Y. Ago, et al., Deficiency of 3-hydroxybutyrate dehydrogenase (BDH1) in mice causes low ketone body levels and fatty liver during fasting, J Inherit Metab Dis. 43 (2020) 960-968. https://doi.org/10.1002/jimd.12243.

[45] A.S. Williams, S.B. Crown, S.P. Lyons, et al., Ketone flux through BDH1 supports metabolic remodeling of skeletal and cardiac muscles in response to intermittent time-restricted feeding, Cell Metab. 36 (2024) 422-437. https://doi.org/10.1016/j.cmet.2024.01.007.

[46] D.B. Stagg, J.R. Gillingham, A.B. Nelson, et al., Diminished ketone interconversion, hepatic TCA cycle flux, and glucose production in D-β-hydroxybutyrate dehydrogenase hepatocyte-deficient mice, Mol. Metab. 53 (2021) 101269. https://doi.org/10.1016/j.molmet.2021.101269.

[47] J.D. McGarry, D.W. Foster, Regulation of hepatic fatty acid oxidation and ketone body production, Annu Rev Biochem. 49 (1980) 395-420. https://doi.org/10.1146/annurev.bi.49.070180.002143.

[48] E.O. Balasse, F. Fery, Ketone body production and disposal: effects of fasting, diabetes, and exercise, Diabetes Metab Rev. 5 (1989) 247-270. https://doi.org/10.1002/dmr.5610050304.

[49] S.E. Hall, M.E. Wastney, T.M. Bolton, et al., Ketone body kinetics in humans: the effects of insulin-dependent diabetes, obesity, and starvation, J Lipid Res. 25 (1984) 1184-1194. https://www.ncbi.nlm.nih.gov/pubmed/6440941

[50] S. Rubler, J. Dlugash, Y.Z. Yuceoglu, et al., New type of cardiomyopathy associated with diabetic glomerulosclerosis, Am J Cardiol. 30 (1972) 595-602. https://doi.org/10.1016/0002-9149(72)90595-4.

[51] A.E. Wentz, D.A. d'Avignon, M.L. Weber, et al., Adaptation of myocardial substrate metabolism to a ketogenic nutrient environment, J Biol Chem. 285 (2010) 24447-24456. https://doi.org/10.1074/jbc.M110.100651.